ЯДЕРНА ФІЗИКА ТА ЕНЕРГЕТИКА / NUCL. PHYS. AT. ENERGY 27 (2026) 219–227 ISSN 1818-331X

ЯДЕРНА ФІЗИКА
NUCLEAR PHYSICS

УДК 539.172.17 https://doi.org/10.15407/jnpae2026.03.219

T. J. Abd Alhessien*, F. A. Majeed

Department of Physics, College of Education for Pure Sciences, University of Babylon, Babylon, Iraq

*Corresponding author: thaeir.alkawwaz@gmail.com

COUPLED-CHANNEL AND SEMICLASSICAL ANALYSIS OF ^{4,6,8}He + ^{197}Au FUSION NEAR THE COULOMB BARRIER

Fusion of ^{4,6,8}He + ^{197}Au has been investigated near and below the Coulomb barrier. Three complementary approaches were employed: (i) a quantum coupled-channels (CC) framework (with continuum discretized coupled-channels when breakup was relevant), (ii) a semiclassical treatment of the relative motion, and (iii) the Wong single-parabolic-barrier formula. The fusion cross-section σ_{fus}, barrier distribution $D_{fus} = d^2(E\sigma_{fus})/dE^2$, and fusion probability P_{fus} were computed. Couplings to collective excitations and transfer/breakup channels were incorporated through the coupling matrix, while barrier transmission was evaluated via Wentzel–Kramers–Brillouin penetrabilities. These couplings were shown to broaden the effective barrier distribution and to enhance sub-barrier tunneling relative to a one-barrier picture. Across all systems, the quantum CC description was found to reproduce the data most accurately, the semiclassical model was observed to capture the main systematics, and the Wong formula was used chiefly above the barrier as a baseline. In this way, the joint roles of nuclear structure and reaction dynamics in shaping fusion observables were delineated for light-on-heavy systems.

Keywords: fusion reaction, elastic and inelastic scattering, low and intermediate energy, heavy-ion reactions, nuclear reaction models and methods.

1. Introduction

The remarkable development in the field of nuclear fusion, which has emerged in recent decades and coincided with the great development in the field of laboratory nuclear experiments, astrophysics, and clean energy, has contributed significantly to the development and understanding of the behavior of low-energy nuclei. The probability of a nuclear reaction resulting from the exchange of nucleons between the projectile and the target was the primary factor in the formation of the nuclear system and the determination of the Coulomb barrier. Determining the paths and outcomes of the reaction rests on the responsibility of angular momentum, which has a direct impact on the probability of fusion between the reactants, the methods used in transport, and the nuclear spectrum. As a result, the fundamental role of the internal nuclear structure in shaping and directing the reaction dynamics and how to control the reactants during nuclear fusion has emerged in a pivotal manner [1–4]. Current research is not limited to the traditional laboratory environment but has been able to simulate prevailing conditions such as those of stars and planets. This has contributed to the acquisition of extensive experimental data on a large scale and has had a significant impact on improving the accuracy of theoretical fusion models [5]. One of the results that scientists have been able to obtain is the reconstruction of mathematical foundations closely related to the creation of nuclei and the development of stars over cosmic time. This has enabled scientists to gain a deep understanding of all the mechanisms controlling nuclear fusion within fusion-based environments. As previously noted, fusion is one of the primary options for providing energy for future generations because it offers several advantages that distinguish it from other resources, including the lack of radioactive pollutants compared to fission, as well as the availability of its resources and environmental sustainability. Scientists have successfully produced energy from fusion that exceeds the energy produced by lasers at the National Ignition Facility in the United States [6]. This was the first step in transforming fusion into a practical concept after it had been limited to theory. Achievements are accelerating and are underway to establish infrastructure for nuclear fusion. China was a pioneer in setting a timetable for the next decade to establish the first industrial reactor and market it during the first half of the current century [7]. Meanwhile, pioneering programs such as the SPARC project, which leverages high-temperature superconductivity technologies, are expected to achieve net energy gains within two years [8]. This could represent a critical turning point, moving fusion research from the laboratory experiment stage to the horizons of real-world industrial applications. In recent years, there has been an increasing number of detailed and large-scale research efforts, both theoretical and experimental, to shed light on the effects of the disintegration of weakly bound nuclei on the prospects of nuclear fusion [8, 9]. For the first time, it has become possible to track collision dynamics from the first moment of contact until the complete overlap of the nuclear density distributions of the interacting nuclei, a level of understanding previously unavailable for other classical nuclear reactions [6, 8]. The study of nuclear fusion is of strategic importance, as it is considered a pivotal step in the formation of superheavy isotopes, which have great future application potential and significant scientific importance in astrophysics [6]. Computational progress has made it possible to approximate the continuum in describing these reactions through advanced simulations of quantum coupled-channels (CC) using the continuum discretized coupled-channels (CDCC) framework [9, 10]. Comparisons between semiclassical calculations and quantum models have shown that combining these two approaches provides a solid basis for predicting nuclear fusion behavior, especially at energies around the Coulomb barrier V_b [9]. As for the formula, heavy ions were studied in detail, and an analytical formula was developed that links the fusion cross-section (σ) to the collision energy (E) based on the properties of the nuclear barrier [11]. This work aimed to investigate and quantify how coupling effects such as collective excitations, transfer, and breakup have influenced the fusion behavior of the systems ^{4,6,8}He + ^{197}Au near and below the Coulomb barrier by applying and benchmarking three theoretical approaches: the quantum CC/CDCC framework, the semiclassical model, and the Wong formula, in direct comparison with experimental observations.

The present work extends a preliminary study by Abd Alhessien and Majeed [12], which analyzed the ^{8}He + ^{197}Au system using a basic CC framework, by incorporating all three helium isotopes (A = 4, 6, 8) within a unified CDCC-based framework augmented by a semiclassical treatment. That earlier study did not include ^{4}He and ^{6}He projectiles, barrier distributions, or the three-way CC/SCF/Wong benchmark analysis provided here. The extension to the complete isotopic chain and the systematic comparison of σ_{fus}, D_{fus}, and P_{fus} constitute the primary novelties of the present manuscript.

2. Theoretical part

2.1. Coupling channel formalism

Heavy-ion interactions in medium-mass systems are generally described using a semiclassical approach [13]. This approach assumes that the fusion cross-section is sensitive to large angular momentum (l) values, and that the relative motion possesses a very small wavelength corresponding to the center-of-mass motion of the nuclei [13, 14]. In reality, initial internal excitations and particle-transfer mechanisms can significantly alter the fusion cross-section of the colliding nuclei. Therefore, several degrees of freedom contributing to the dynamic reaction must be incorporated [15]. The present work aimed to apply an appropriate theoretical framework to address this issue – the coupled-channel technique. However, its implementation becomes particularly complex when applied to breakup channels, especially for weakly bound nuclei, as they include an infinite continuum of unbound states. In practice, this continuum is approximated by a finite set of discretized states within the CDCC method [16]. In the collision process, **r** denotes the relative separation vector between the projectile and target, while ξ_P and ξ_T represent the intrinsic coordinates describing the internal structures of the projectile and target, respectively. Accordingly, the total Hamiltonian of the system can be expressed as [17, 18]:

$$H = T(\mathbf{r}) + hP_p(\xi P_p) + h_T(\xi_T) + V(r, \xi_P, \xi_T)\,. \quad (1)$$

The term $T(\mathbf{r})$ represents the relative motion between the two interacting masses and the center of mass of the colliding nuclei, while $h_P(\xi_P)$ and $h_T(\xi_T)$ describe the internal states of the projectile and target, respectively. The potential $V(r, \xi_P, \xi_T)$ expresses the interaction among all degrees of freedom [17]. The corresponding time-dependent coefficients or eigenvector amplitudes are defined by [17, 18]:

$$a_\alpha(t) = \langle \phi_\alpha \,|\, \Psi(t) \rangle\,. \quad (2)$$

The Alder and Winther method has been developed to study Coulomb excitation involving the treatment of the motion of the relative by classical mechanics for the potential where is the lowest energy (ground state) by using the projectile trajectory, while the inherent motion has been processed. In the quantum-mechanical description, Coulomb excitation is treated as a time-dependent problem, where the time-dependent Schrödinger equation governs the evolution of the nuclear wave function under the influence of the time-dependent Hamiltonian [16, 19]. The Schrödinger equation is used to solve for the wave function depending on the Hamiltonian over time, and the wave function for an excitable nucleus [17]

$$H(t)\Psi(t) = i\hbar \frac{\partial}{\partial t}\Psi(t)\,. \quad (3)$$

The total wave function is expanded in terms of the intrinsic eigenstates of the system as

$$\Psi(t) = \sum_\alpha a_\alpha(t)\phi_\alpha\,, \quad (4)$$

where $a_\alpha(t)$ are the time-dependent amplitudes associated with the intrinsic states ϕ_α. Substituting this expansion into the time-dependent Schrödinger equation yields the set of coupled Alder–Winther (AW) equations [10]:

$$\frac{d}{dt}a_\alpha(t) = -\frac{i}{\hbar}\sum_\beta V_{\alpha\beta}(t)e^{-i\omega_{\alpha\beta}t}a_\beta(t). \quad (5)$$

The initial conditions for these equations correspond to the moment of collision, where the projectile is assumed to be in its ground state. The final population of channel α in a collision with angular momentum *l* determines the probability of transition between coupled states. The corresponding reaction cross-section is given by [18]:

$$\sigma_\alpha = \sum(1+2l)\ p_\alpha(l,E), \quad (6)$$

where $p_\alpha(l,E)$ is the transition probability for channel α at a given energy *E*. The AW formalism can be extended to evaluate the fusion cross-section by expressing it in general form for multichannel scattering as [2]

$$\sigma_{\text{fus}}(E) = \sum_l (2l+1)T_l(E), \quad (7)$$

where $T_l(E)$ denotes the transmission coefficient for each partial wave *l*. The fusion probability for a given partial wave α is defined as [2]

$$P_\alpha(l,E) = \frac{4K}{\hbar v}\int_0^\infty W_\alpha(r)\left|u_\alpha^l(k,r)\right|^2 dr, \quad (8)$$

where $u_\alpha^l(k,r)$ is the radial wave function of channel α, and $W_\alpha(r)$ is the imaginary part of the optical potential, representing absorption into the fusion channel. Within this approximation, the AW method provides a reliable framework for evaluating the fusion cross-section [10]

$$T_l(E) \approx exp\left[-2\int_{r_1}^{r_2}\sqrt{\frac{2\mu}{\hbar^2}(V_{eff}(r)-E)}\ dr\right]. \quad (9)$$

As the particle mass decreases, the probability of tunneling through the potential barrier increases. Consequently, the system is expected to be localized at a point closest to the classical trajectory within the channel. The description of the coupling channels method is in [4]. The colliding nuclei are described with the collective properties taken into consideration. However, this approach is complex, especially when we calculate the Hamiltonian coupling, and to obtain an approximate solution to estimate cross-sections of fusion. By a semiclassical field, for two spherical nuclei colliding, the penetrability probability can be estimated utilizing the approximation for the Wentzel–Kramers–Brillouin (WKB) that reads [18]

$$T_l^{(K)}(E) = \left[1+\exp\left(\frac{2\pi\left(V_b(l)-E\right)}{\hbar\omega}\right)\right]^{-1}, \quad (10)$$

and indicate the internal and external classical turning points to achieve the relationship. There is an improved version so far that introduces Kemble's transmission probability expression [18] in regard to the equivalent barrier, which is useful for energy above the barrier. It is given by

$$V_{tot}(r) = V_C(r) + V_N(r) + \frac{\hbar^2\left(l^2+1\right)}{2\mu r^2}, \quad (11)$$

$$V_N(r) = -\frac{V_0}{1+\exp\left[r/a - R_0/a\right]}, \quad (12)$$

$$R_0 = r_0\sqrt[3]{A_P + A_T}. \quad (13)$$

The parameters of radius and the parameter of diffuseness *a* are the same as in the potential of AW. The one-dimensional WKB approximation has been used to estimate the cross-section in the merger. In other studies, other analytical approximations have been used, for example, the Wong formula taken from the Hill–Wheeler approximation (a parabolic inverse approximation for the barrier top) [17, 18].

2.2. Fusion barrier distribution

From the theoretical viewpoint, the formalism of CC is the traditional method for addressing the effect of coupling between the relative motion and the nuclear substantial degrees of freedom. This involves couplings to static disfigurement, states of vibrational, and also transfer and breakup channels. In the case of many medium-mass nuclei, the coupling strength is greater and needs to involve terms of the expansion of the higher-order potential of coupling [5]. For reactions involving rotating nuclei, the geometric model predicts that continuously distributed fusion barriers have replaced the one-dimensional Coulomb barrier of one dimension, which corresponds to the alternate orientations of the target and projectile nucleus. The total cross-section of fusion is expressed by an integration over a continuous barrier distribution [17, 18]

$$\sigma_{fus}(E) = \int_0^\infty f(B)\sigma_W(E;B)dB. \quad (14)$$

The final equation delineates the distribution of barriers, with the magnitude of the potential barrier exhibiting a direct proportionality to this parameter.

The cross-sectional representation provided by the Weng approximation yields a closed distribution

$$f\left(B\right)=\frac{1}{\sqrt{2\pi}\Delta}\exp\left(-\frac{\left(B-B_0\right)^2}{2\Delta^2}\right). \quad (15)$$

One obtains,

$$D_{fus}\left(E\right)=\frac{d^2}{dE^2}\left[E\sigma_{\text{fus}}\left(E\right)\right]. \quad (16)$$

Classically, the function of Fermi can be roughly approximated by a step function, while its derivative corresponds to the Dirac delta function

$$\frac{d}{dE}\left(\frac{1}{1+e^{(E-E_0)/\Delta}}\right)\to\delta\left(E-E_0\right) \quad (17)$$

and denoted the radius and height of the potential barrier [15]. It is possible to extract the barrier distribution from the experimental and excitation-calculated functions by multiplying (E) by (σ_{CM}) and deriving twice with respect to (E), denoting the cross-section of fusion and energy in the center-of-mass frame [5, 19]. The point difference method was used to calculate it numerically in the case of data with steps of equivalent energy steps, i.e.,

$$D_{\text{fus}}\left(E_i\right)\approx\frac{E_{i+1}\sigma_{i+1}-2E_i\sigma_i+E_{i-1}\sigma_{i-1}}{\left(\Delta E\right)^2}, \quad (18)$$

where the evaluation is done at energies using steps of different energies, whereas

$$D_{\text{fus}}\left(E_i\right)\approx\frac{E_{i+1}\sigma_{i+1}-E_i\sigma_i}{E_{i+1}-E_i}-\frac{E_i\sigma_i+E_{i-1}\sigma_{i-1}}{E_i-E_{i-1}}. \quad (19)$$

Approximately, the error in the statistics is related to the energy via the second derivative, which is given by

$$\delta D\sim\frac{\delta\sigma}{\left(\Delta E\right)^2}, \quad (20)$$

represented is the absolute uncertainty in the cross-section.

2.3. Wong formula

One of the most important relations in heavy-ion fusion physics is the Wong formula, which is used to calculate the fusion cross-section at energies close to the Coulomb barrier. The general expression for the fusion cross-section is given by

$$\sigma_{\text{fus}}\left(E\right)=\frac{\pi}{k^2}\sum_{l=0}^{\infty}(2l+1)T_l\left(E\right), \quad (21)$$

where $T_l\left(E\right)$ denotes the transmission (penetration) probability for a partial wave l. The total potential barrier is assumed to be parabolic near its maximum and can be approximated as

$$V_l\left(r\right)\approx V_b+\frac{1}{2}\mu\omega^2\left(r-R_b\right)^2+\frac{\hbar^2\left(l^2+1\right)}{2\mu R_b^2}, \quad (22)$$

where V_b and R_b are the height and radius of the Coulomb barrier, respectively. This approximation allows for an analytic solution of the barrier penetrability using the Hill–Wheeler formula:

$$T_l(E)=\frac{1}{1+\exp\left[\frac{2\pi\left(V_b(l)-E\right)}{\hbar\omega}\right]} \quad (23)$$

with the barrier height for each partial wave given by

$$V_b\left(l\right)=V_b+\frac{\hbar^2\left(l^2-l\right)}{2\mu R_b^2}. \quad (24)$$

Integrating over all partial waves yields the final form of the Wong formula [11]:

$$\sigma_{Wong}\left(E\right)=\frac{\hbar\omega R_b^2}{2E}\ln\left[1+\exp\left(\frac{2\pi\left(E-V_b\right)}{\hbar\omega}\right)\right]. \quad (25)$$

3. Results and discussion

This study focuses on the analysis of fusion reactions associated with stable corona nuclei by calculating the fusion cross-section, the barrier distribution, and the barrier penetration probability, using the CDCC approach. The formulation of the interaction potential is done using the Woods–Saxon model by separating the imaginary and real components that represent the separation channels of the coupling diagram. For the analysis to be consistent, all parameters (diffusion coefficient, depth, and radius) must be extracted from the diagonal matrix components of the interaction potential, which are included in the algorithm for CC. As a result, this provides us with a picture for describing the nuclear dynamics. This ensures that the geometric properties of the nuclear potential are consistent with the experimental data by reproducing the Coulomb-barrier height and radius predicted by the Akyüz–Winther potential [20], as shown in the Table. The theoretical results are represented in the accompanying figures by characteristic curves: solid or dashed red and blue curves, respectively, and the solid green curves represents the Wong formula. Representing the fusion cross-section (mb), the barrier distribution (mb/MeV), and the penetration probability, these representations demonstrate the difference between calculations derived from a fully quantum mechanical CC code and those derived from a semi-classical code-based (SCF) model. The red arrow on the x-axis of each figure marks the position of the Coulombic barrier, which serves as a reference for distinguishing between fusion properties below and above the Coulomb barrier.

The parameters of the Akyüz–Winther potential with the associated Coulomb barrier heights for the systems

Systems	V_0, MeV	r_0, fm	a_0, fm	W_i, MeV	r_i, fm	a_i, fm	V_b, MeV
^{4}He + ^{197}Au	–135.9	1.030	0.850	–45.3	0.920	0.788	18.69
^{6}He + ^{197}Au	–192.9	1.100	0.700	–64.3	0.929	0.783	18.13
^{8}He + ^{197}Au	–161.0	0.950	0.760	–54.1	0.938	0.777	17.71

3.1. ^{4}He + ^{197}Au system

Fig. 1 shows a detailed comparison between experimental results and theoretical predictions for the thallium ^{4}He + ^{197}Au fusion reaction, highlighting the crucial role of channel coupling and the importance of the Wong formula in interpreting fusion dynamics. At the Coulomb barrier energy 18.69 MeV, panel (*a*) shows that the Wong curves (*solid green*), assuming a single parabolic barrier, provide a relatively good match to the cross-section σ_{fus} at energies above the barrier and are not significantly affected by the internal structure of the nuclei. However, this formula, by its nature, fails to capture the large experimental increase in the cross-section at energies below the barrier, as it completely ignores the actual barrier propagation due to channel coupling. Conversely, coupled calculations (CC in *solid red* and SCF in *solid blue*) show that integration of the internal couplings leads to enhanced quantum tunneling under the barrier, accurately explaining the higher integration cross-sections compared to the experimental results (*black circles*). In panel (*b*), the distribution of the barrier D_{fus} has been calculated. The Wong formula is narrow and symmetrical, and the shape reflects the assumption of a constant barrier, while the calculations of the coupled quantum model are more variable and broader. The peak is very clear and in good agreement with the data. The results demonstrate the intrinsic nature of the nuclear interactions and the resulting interference between the degrees of freedom resulting from fusion. The CC and SCF models highlight the physical property of fusion, while these coupling properties are absent in the Wong formula. Panel (*c*) shows that the fusion probability P_{fus} according to the Wong formula gradually rises. This difference confirms that the Wong formula only provides an "average" description of the behaviour, but cannot describe channel coupling and is insufficient to explain the general dynamics. However, they fail below and above the barrier, neglecting the role of quantum interference and internal couplings that reshape the barrier spectrum. In contrast, the CC framework (using CC and SCF) provides a deeper and more comprehensive representation, able to capture the complex effects of nuclei, enhancing the effectiveness of CDCC as a theoretical tool for accurately simulating heavy ion fusion when compared to laboratory results.

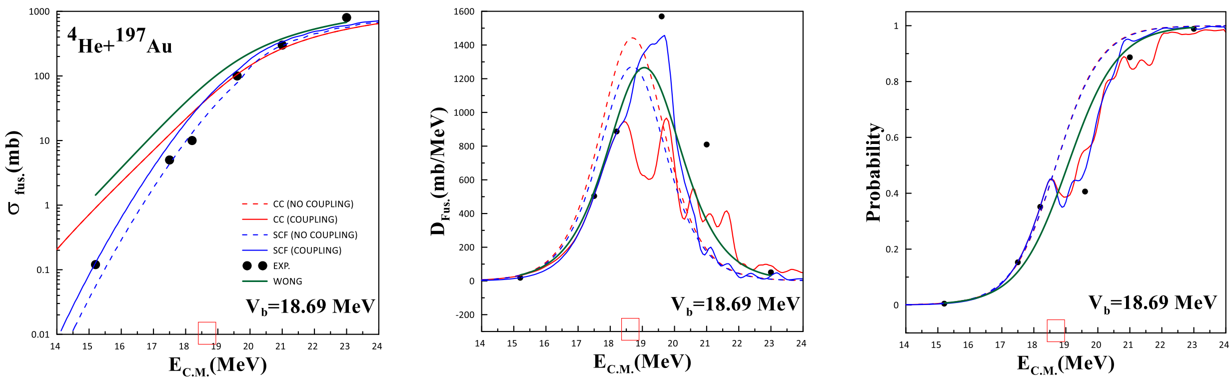

a *b* *c*

Fig. 1. Comparison of the excitation function calculations of the cross-sections (σ_{fus}), barrier distributions (D_{fus}) and probability (P_{fus}) in the semiclassical mechanical SCF code (*blue curves*), the quantum mechanical CC code (*red curves*) and the Wong formula (*green curves*) with the laboratory data (*solid circles*) [21] for the ^{4}He + ^{197}Au system. (See color Figure on the journal website.)

The divergence between the semiclassical (SCF) and quantum CC calculations when channel couplings are active arises because the SCF model treats the relative nuclear motion classically along a trajectory, thereby suppressing quantum interference effects between partial waves in the sub-barrier region. Such interference is fully retained in the quantum CC/CDCC formalism and becomes dominant near and below V_b. As a consequence, the two approaches converge at energies well above V_b (where the WKB approximation is valid) but diverge once the coupling-enhanced tunneling regime is entered. The overestimation of σ_{fus} above the barrier by all CC calculations is attributed to the incomplete channel space: pre-equilibrium emission, incomplete fusion, and direct breakup into the continuum all provide additional flux-absorption pathways above V_b that are not explicitly included in the current CC/CDCC framework. Incorporating these channels in future work is expected to improve the above-barrier description.

3.2. ^{6}He + ^{197}Au system

Fig. 2 clearly shows the agreement of the coupled quantum framework (CC, *red curves*) in the description of the fusion dynamics of ^{6}He + ^{197}Au, at all energies and below the Coulomb barrier $V_b \approx 18.612$ MeV, as well as the semi-classical model (SCF, *blue curves*) and the Wong equation curve (Wong, *green curves*). In panel (*a*), the predictions of σ_{fus} improve markedly when channel coupling is introduced into the CC and SCF calculations, and these curves become closer to the experimental data (*black dots*), while the Wong formula provides a good description only at energies above and below the barrier. This is because the Wong equation relies on approximately a single equivalent barrier (a parabolic approximation of the barrier) and ignores coupling, decoupling, and halo properties in ^{6}He. Therefore, it is able to give an average value for the penetration rate in the classical band above the barrier but severely underestimates σ_{fus} when multichannel quantum phenomena (coupling-enhanced tunneling, decay, and mass transfer) are dominant below the barrier. The effect of coupling is clearly demonstrated in panel (*b*), where CC produces a broad Gaussian-shaped barrier distribution D_{fus} that matches the contours of the experimental distribution, while the Wong equation produces a narrow, single-peaked distribution due to its assumption of a fixed barrier. This barrier fragmentation is what broadens the range of energies at which fusion is likely for coupled models. Panel (*c*) shows that the fusion probability P_{fus} in the CC frame transitions smoothly and mimics the abrupt rise and saturation observed experimentally, while the Wong curve shows a slower rise for the corona and coupling effects. In conclusion, the Wong equation becomes a useful reference as a single-barrier model at energies above the barrier, but to understand and quantify the effects of corona nuclei and coupling below the barrier, CC models such as CDCC are required, as confirmed by the measured results in [22].

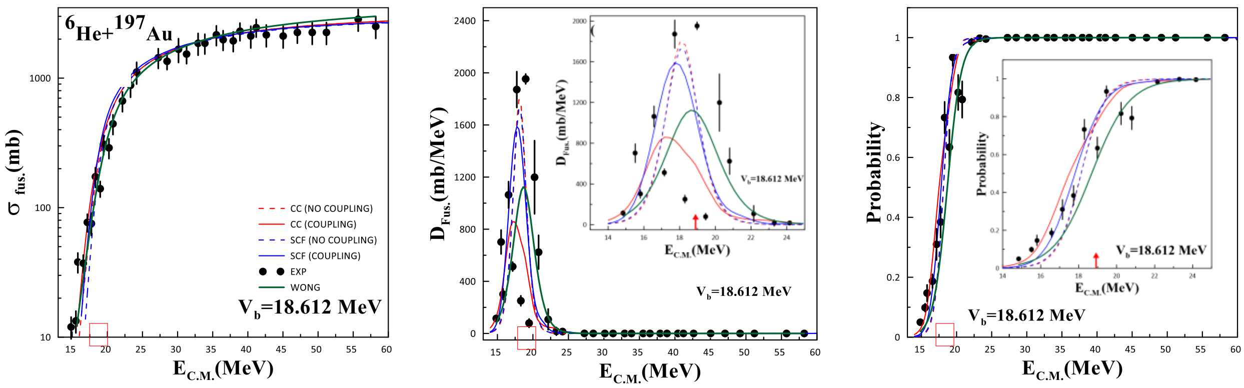

a *b* *c*

Fig. 2. Comparison of the excitation function calculations of the cross-sections (σ_{fus}), barrier distributions (D_{fus}) and probability (P_{fus}) in the semiclassical mechanical SCF code (*blue curves*), the quantum mechanical CC code (*red curves*) and the Wong formula (*green curves*) with the laboratory data (*solid circles*) [22] for the ^{6}He + ^{197}Au system. (See color Figure on the journal website.)

The near-coincidence of the CC (no coupling) and CC (coupling) curves in panel (*b*) for the ^{6}He + ^{197}Au system is a genuine physical result. ^{197}Au has a modest oblate quadrupole deformation $\beta_2 \sim -0.13$ [23] and a relatively high first 2^+ excitation energy ~547 keV, so the Coulomb coupling matrix elements connecting the ground state to collective target states are comparatively weak for a light projectile such as ^{6}He. Furthermore, the dominant coupling effects for ^{6}He + ^{197}Au originate from the halo/di-neutron structure of ^{6}He itself (breakup and two-neutron transfer channels), which broaden the barrier distribution through projectile-driven mechanisms. The mild target deformation therefore produces little additional change relative to the already strong projectile-driven coupling. The coupling matrix elements have been verified numerically, and the near-coincidence is confirmed to be a physically expected result, not a computational artifact.

3.3. $^{8}He + ^{197}Au$

Fig. 3 shows a close comparison of the interaction $^{8}He + ^{197}Au$ between experimental results and theoretical calculations using different models: the CC model (CC, *red curves*), the semi-classical model (SCF, *blue curves*), and the Wong formula (Wong, *green curves*). In panel (*a*), the fusion cross-section σ_{fus} shows that the CC model achieves close agreement with the experimental values, especially at energies below and above the barrier V_b = 20.187 MeV. While the Wong curve appears to describe the data acceptably only at energies above the barrier, it assumes a single parabolic barrier with a constant curvature, which neglects the fragile structure and neutron corona in ^{8}He and the effects of transport and dissociation channels. However, this formula fails to reproduce the large increase in the cross-section at sub-barrier energies, where multichannel quantum phenomena (halo-enhanced tunneling and deconvolution couplings) dominate. Panel (*b*) highlights the barrier distribution D_{fus}. CC presents a broad, multi-peaked distribution reflecting barrier fragmentation caused by dynamical couplings, while the Wong distribution remains narrow and single-peaked because it assumes a constant barrier. This feature reflects that effective barriers in halo systems are not unique, but are distributed over a wide range of energies. In panel (*c*), the coalescence probability P_{fus} exhibits a smoother transition in the CC framework, clearly mimicking the abrupt increase and saturation measured experimentally, while the Wong curve remains slower and less expressive of these properties. This highlights the pivotal role of the neutron corona in ^{8}He, which promotes tunneling and increases the probability of fusion at low energies. In conclusion, the Wong formula is a useful reference for estimating behavior above the barrier, but it is insufficient in weakly bound systems, where CC models (such as CC and CDCC) become necessary to accurately characterize the interactions of heavy ions with halo nuclei. These results, as in [24], confirm that ignoring the effects of coupling and the internal structure of the corona leads to a fundamental shortcoming of simplified models, especially in the near-energy range and below the Coulomb barrier.

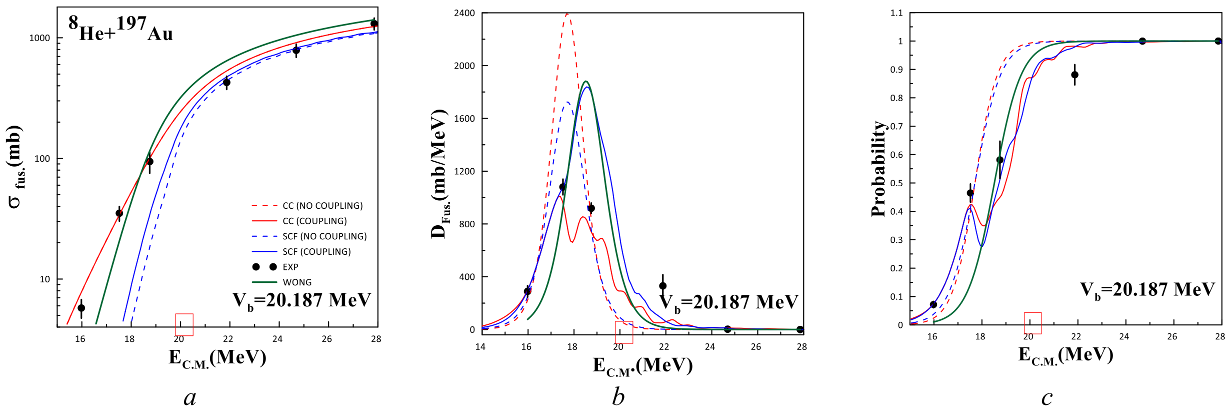

Fig. 3. Comparison of the excitation function calculations of the cross-sections (σ_{fus}), barrier distributions (D_{fus}), and probability (P_{fus}) in the semiclassical mechanical SCF code (*blue curves*), the quantum mechanical CC code (*red curves*), and the Wong formula (*green curves*) with the laboratory data (*solid circles*) [24] for the $^{8}He + ^{197}Au$ system. (See color Figure on the journal website.)

The divergence between CC (coupling) and the Wong formula above V_b in the $^{8}He + ^{197}Au$ system (panel (*a*)) arises because the Wong formula assumes a single static parabolic barrier producing a smooth monotonic $\sigma_{fus}(E)$. When channel couplings are active in the CC calculation even above V_b, flux redistribution into transfer and breakup channels modifies the effective transmission coefficients $T_l(E)$ for each partial wave. For ^{8}He specifically, the four-valence-neutron halo extends the nuclear density well beyond the nominal radius, coupling the CDCC continuum states to the elastic channel throughout the measured energy range. This makes the coupling-corrected fusion cross-section sensitive to breakup effects at all energies, not only below V_b, producing the observed departure from the bare Wong curve above the barrier.

The inclusion of coupling effects substantially improves the reproduction of the sub-barrier fusion cross-section and the shape of the barrier distribution relative to single-barrier models. However, non-negligible discrepancies between theory and experiment remain, particularly above the Coulomb barrier in the $^{4}He + ^{197}Au$ system and in the barrier distribution panel of Fig. 1, *b*, where all theoretical calculations deviate from the measured data. These residual deviations suggest that additional reaction channels such as pre-equilibrium emission, incomplete fusion, and compound-nucleus evaporation corrections need to be incorporated in future, more complete calculations.

4. Conclusions

This study reveals the essential role of channel coupling in achieving accurate simulations of heavy ion fusion reactions at energies close to the Coulomb barrier for the systems ^{4}He + ^{197}Au, ^{6}He + ^{197}Au, and ^{8}He + ^{197}Au. Based on the CDCC approach and within the framework of both semiclassical and quantum descriptions, as well as the Wong formula based on the potential $Tl(E)$, an in-depth analysis of the cross-sections σ_{fus}, the barrier distributions D_{fus}, and the fusion probabilities P_{fus} was performed, along with a systematic comparison with available experimental data. The inclusion of coupling effects has proven its remarkable ability to improve the agreement between theoretical predictions and experimental results, especially in the energy range above the barrier, where fusion dynamics become more sensitive to nuclear excitations and inelastic interactions. The results indicate that calculations based on CC not only improve the accuracy of the predictions of σ_{fus}, D_{fus}, and P_{fus}, but also accurately reproduce the complex structure of barrier distributions, especially in systems with heavy targets The comparison between the quantum CC and semiclassical SCF models demonstrated the superiority of the quantum model in representing experimental data, and therefore, full reliance should be placed on the quantum model in studying the general properties of fusion. The results demonstrated that the quantum model should be relied upon as a model for studying predictions near the fusion barrier. The effect of merging the CC was very important for interpreting the results and future predictions for future scientific research. Meanwhile, the Wong formula contributed to supporting and understanding the mechanisms of the results and contributing to the development of robust predictive models for nuclear applications.

The authors acknowledge the support from the Department of Physics, College of Education, University of Babylon.

REFERENCES

1. N. Keeley et al. Elastic scattering and reactions of light exotic beams. Prog. Part. Nucl. Phys. 63 (2009) 396.
2. L.F. Canto et al. Recent developments in fusion and direct reactions with weakly bound nuclei. Phys. Rep. 596 (2015) 1.
3. A. Diaz-Torres, I.J. Thompson. Effect of continuum couplings in fusion of halo ^{11}Be on ^{208}Pb around the Coulomb barrier. Phys. Rev. C 65 (2002) 024606.
4. J.J. Kolata, V. Guimarães, E.F. Aguilera. Elastic scattering, fusion, and breakup of light exotic nuclei. Eur. Phys. J. A 58 (2016) 123.
5. F.A. Majeed. The role of the breakup channel on the fusion reaction of light and weakly bound nuclei. Int. J. Nucl. Energy Sci. Technol. 11 (2017) 218.
6. M.H.A. Madhi, F.A. Majeed. Single and coupled channels calculations for fusion reaction of ^{6}Be + ^{209}Bi, ^{11}Be + ^{209}Bi, and ^{15}C + ^{232}Th halo nuclei systems. AIP Conf. Proc. 2398 (2022) 020004.
7. P.R.S. Gomes et al. Fusion, breakup and scattering of weakly bound nuclei at near barrier energies. Open Nucl. Part. Phys. J. 6 (2013) 10.
8. B.B. Back et al. Recent developments in heavy-ion fusion reactions. Rev. Mod. Phys. 86 (2014) 317.
9. S.A. Abbas et al. Fusion reaction study of some selected halo systems. Baghdad Sci. J. 20 (2023) 622.
10. H.L. Harney, P. Braun-Munzinger, C.K. Gelbke. On the semiclassical interpretation of heavy ion reactions. Z. Phys. 269 (1974) 339.
11. C.Y. Wong. Interaction barrier in charged-particle nuclear reactions. Phys. Rev. Lett. 31 (1973) 766.
12. F.A. Majeed, Y.A. Abdul-Hussien. Semiclassical treatment of fusion and breakup processes of ^{6,8}He halo nuclei. J. Theor. Appl. Phys. 10 (2016) 107.
13. F.M. Hussain, F.A. Majeed, M.H. Meteab. Investigation of the calculation of coupled channels for some halo systems. Ukr. J. Phys. 65 (2020) 951.
14. F.M. Hussain, F.A. Majeed, Y.A. Abdul-Hussien. Coupling channels mechanism of complete fusion reactions in some light stable nuclei. AIP Conf. Proc. 2144 (2019) 030003.
15. A.J. Najim, F.A. Majeed, K.H. Al-Attiyah. Improved calculation of fusion barrier distribution. IOP Conf. Ser.: Mater. Sci. Eng. 571 (2019) 012124.
16. F.M. Hussain, F.A. Majeed, Y.A. Abdul-Hussien. Description of coupled-channel in semiclassical treatment of heavy ion fusion reactions. IOP Conf. Ser.: Mater. Sci. Eng. 571 (2019) 012113.
17. R.A. Broglia, A. Winther. Semiclassical theory of heavy ion reactions. Phys. Rep. 4 (1972) 153.
18. L.F. Canto et al. Fusion and breakup of weakly bound nuclei. Phys. Rep. 424 (2006) 1.
19. F.A. Majeed, R.Sh. Hamodi, F.M. Hussian. Effect of coupled channels on semiclassical and quantum mechanical calculations for heavy ion fusion reactions. J. Comput. Theor. Nanosci. 14 (2017) 2242.
20. R.O. Akyüz, A. Winther. Nuclear structure and heavy-ion reactions. In: *Nuclear Structure and Heavy-Ion Reactions*. Proceedings of the International School of Physics "Enrico Fermi", Course LXXVII. R.A. Broglia, C.H. Dasso, R. Ricci (Eds.) (North-Holland, Amsterdam, 1981) p. 491.
21. W.J. Jordan, J.V. Maher, J.C. Peng. The fusion of ^{12}C and ^{16}O with ^{28,29,30}Si. Phys. Lett. B 87 (1979) 38.
22. Yu.E. Penionzhkevich et al. Excitation functions of fusion reactions and neutron transfer in the interaction of ^{6}He with ^{197}Au and ^{206}Pb. Eur. Phys. J. A 31 (2007) 185.
23. P. Möller et al. Nuclear ground-state masses and deformations: FRDM (2012). At. Data Nucl. Data Tables 109–110 (2016) 1.
24. A. Lemasson et al. Modern Rutherford experiment: Tunneling of the most neutron-rich nucleus. Phys. Rev. Lett. 103 (2009) 232701.

Т. Дж. Абд Альхессієн*, Ф. А. Маджід

Кафедра фізики, Коледж природничих наук, Вавилонський університет, Вавилон, Ірак

*Відповідальний автор: thaeir.alkawwaz@gmail.com

АНАЛІЗ ЗЛИТТЯ ЯДЕР ^{4,6,8}He З ^{197}Au ПОБЛИЗУ КУЛОНІВСЬКОГО БАР'ЄРА МЕТОДОМ ЗВ'ЯЗАНИХ КАНАЛІВ ТА В НАПІВКЛАСИЧНОМУ ПІДХОДІ

Досліджено процес злиття ядер ^{4,6,8}He з ^{197}Au в діапазоні енергій поблизу кулонівського бар'єра та нижче нього. Застосовано три взаємодоповнювальні підходи: (i) квантовий формалізм зв'язаних каналів (CC) (включно з методом зв'язаних каналів з дискретизацією неперервного спектра для випадків, коли суттєвим був процес розвалу ядра), (ii) напівкласичний опис відносного руху та (iii) формула Вонга для моделі єдиного параболічного бар'єра. Було розраховано переріз злиття σ_{fus}, розподіл бар'єрів $D_{\text{fus}} = d^2(E\sigma_{\text{fus}})/dE^2$ та ймовірність злиття P_{fus}. Взаємозв'язок з колективними збудженнями та каналами передачі нуклонів чи розвалу ядра враховувався через матрицю зв'язку, тоді як проходження крізь бар'єр оцінювалося за допомогою коефіцієнтів проникності, розрахованих у наближенні Вентцеля–Крамерса–Бріллюена. Показано, що ці взаємозв'язки призводять до розширення ефективного розподілу бар'єрів та підсилення підбар'єрного тунелювання порівняно з моделлю єдиного бар'єра. Встановлено, що для всіх розглянутих систем квантовий опис у рамках методу зв'язаних каналів забезпечує найвищу точність відтворення експериментальних даних; напівкласична модель адекватно описує основні закономірності процесу, а формула Вонга використовується переважно як базовий орієнтир для енергій вище бар'єра. Таким чином, визначено спільний вплив ядерної структури та динаміки реакції на характеристики процесу злиття в системах, що складаються з легкого та важкого ядер.

Ключові слова: реакція злиття, пружне та непружне розсіяння, низькі та проміжні енергії, реакції за участю важких іонів, моделі та методи ядерних реакцій.

Надійшла / Received 21.10.2025